Effective Hypothermic Storage of Human Pluripotent Stem Cell-Derived Cardiomyocytes Compatible With Global Distribution of Cells for Clinical Applications and Toxicology Testing

CLÁUDIA CORREIA,[a,b] ALEXEY KOSHKIN,[a,b] MADALENA CARIDO,[a,b] NUNO ESPINHA,[a,b] TOMO ŠARIĆ,[c] PEDRO A. LIMA,[d] MARGARIDA SERRA,[a,b] PAULA M. ALVES[a,b]

[a]Instituto de Tecnologia Química e Biológica António Xavier, Universidade Nova de Lisboa, Oeiras, Portugal; [b]iBET, Instituto de Biologia Experimental e Tecnológica, Oeiras, Portugal; [c]Center for Physiology and Pathophysiology, Institute for Neurophysiology, Medical Faculty, University of Cologne, Cologne, Germany; [d]Nova Medical School, Universidade Nova de Lisboa, Lisboa, Portugal

Correspondence: Margarida Serra, Ph.D., Animal Cell Technology Unit, Instituto de Biologia Experimental e Tecnológica and Instituto de Tecnologia Química e Biológica António Xavier, Apartado 12, 2781-901 Oeiras, Portugal. Telephone: 351 21 446 94 31; E-Mail: mserra@ibet.pt

ABSTRACT

To fully explore the potential of human pluripotent stem cell-derived cardiomyocytes (hPSC-CMs), efficient methods for storage and shipment of these cells are required. Here, we evaluated the feasibility to cold store monolayers and aggregates of functional CMs obtained from different PSC lines using a fully defined clinical-compatible preservation formulation and investigated the time frame that hPSC-CMs could be subjected to hypothermic storage. We showed that two-dimensional (2D) monolayers of hPSC-CMs can be efficiently stored at 4°C for 3 days without compromising cell viability. However, cell viability decreased when the cold storage interval was extended to 7 days. We demonstrated that hPSC-CMs are more resistant to prolonged hypothermic storage-induced cell injury in three-dimensional aggregates than in 2D monolayers, showing high cell recoveries (>70%) after 7 days of storage. Importantly, hPSC-CMs maintained their typical (ultra)structure, gene and protein expression profile, electrophysiological profiles, and drug responsiveness. STEM CELLS TRANSLATIONAL MEDICINE 2016;5:658–669

SIGNIFICANCE

The applicability of human pluripotent stem cell-derived cardiomyocytes (hPSC-CMs) in the clinic/industry is highly dependent on the development of efficient methods for worldwide shipment of these cells. This study established effective clinically compatible strategies for cold (4°C) storage of hPSC-CMs cultured as two-dimensional (2D) monolayers and three-dimensional (3D) aggregates. Cell recovery of 2D monolayers of hPSC-CMs was found to be dependent on the time of storage, and 3D cell aggregates were more resistant to prolonged cold storage than 2D monolayers. Of note, it was demonstrated that 7 days of cold storage did not affect hPSC-CM ultrastructure, phenotype, or function. This study provides important insights into the cold preservation of PSC-CMs that could be valuable in improving global commercial distribution of hPSC-CMs.

INTRODUCTION

The emerging potential of human pluripotent stem cell-derived cardiomyocytes (hPSC-CMs) in cell-based cardiac repair, patient-specific disease modeling, and drug toxicity [1, 2] is strongly pushing these cell-based products toward a global marketplace. To date, many efforts have been made in improving pluripotent stem cell (PSC) expansion [3–6], cardiomyocyte (CM)-lineage differentiation, and enrichment processes [2, 7, 8]; however, little attention has been given to methodologies and protocols to preserve and transport these cell products from the manufacturing site to the clinical setting for immediate administration in patients,

to research institutes, or to biotechnology companies. The complexity is associated with the laborious and time-consuming differentiation protocols, as well as the inability of maintaining the differentiated nonreplicative cells in culture for long periods of time, highlighting the need for developing efficient strategies for preservation of PSC-CMs. The cryopreservation protocols are still highly inefficient, usually resulting in a substantial loss of cell viability and function [9, 10]. Additionally, the majority of these protocols use animal-derived components (e.g., proteins or serum) and/or toxic cryoprotective agents (CPAs; e.g., dimethyl sulfoxide) [11], rendering them unsuitable for clinical applications. It has been demonstrated that serum

residues in the therapeutic product can trigger adverse reactions in patients [12]. Washing protocols are therefore required to remove CPAs, serum, and cellular debris from therapeutic cells before patient administration [11, 12].

Hypothermic preservation can be an alternative to cryopreservation in short-term storage situations (e.g., to perform the intercontinental or transcontinental transport of the cells). During hypothermic storage, cells are maintained at temperatures that range between 4°C and 10°C. These lower temperatures affect cell physiology, namely, by reducing their metabolism, energy storage degradation, and oxygen demand [13]. Effective hypothermic preservation requires the use of preservation solutions that (a) provide optimal concentrations of ions and impermeable molecules to maintain ionic and osmotic balance, (b) prevent the formation of free radicals, (c) maintain an oncotic balance, and (d) supply energy substitutes [14, 15]. A variety of preservation solutions, such as ViaSpan (University of Wisconsin solution), Celsior, Custodiol histidine-tryptophan-ketoglutarate solution and, more recently, HypoThermosol (HTS), were developed taking these factors into consideration [15] and are commercially available today. These solutions showed to be effective for hypothermic storage of a large diversity of cells, tissues, and organs (including neonatal rat ventricular cardiomyocytes [16], renal cells [17], hepatocytes [18, 19], liver tissue [20], synthetic human epidermis tissue [21], kidney [22], pancreas [23], liver [20], and heart [24, 25]). Importantly, some of these formulations can be directly administered into patients, avoiding additional poststorage culture manipulations/costs and washing steps. HTS, for example, has been used as a vehicle solution for different therapeutic cells in several clinical trials, such as in the treatment of autoimmune disorders including rheumatoid arthritis with allogeneic adipose-derived stem cells (NCT01743222), advanced heart failure with myogenic cells (NCT00526253), and restrictive scars using allogeneic dermal fibroblasts (NCT01564407).

The time interval that a cardiac graft can be efficiently cold-stored remains limited to 6 hours [25]. This finite time frame further limits donor heart supply, access, and utility. The ability to efficiently cold-preserve functional CMs for extended periods would provide an appealing off-the-shelf solution for the treatment of cardiac diseases. Several studies have evaluated the ability to preserve adult/neonatal rat/mouse CMs at hypothermic conditions [16, 26–29]. For example, Snyder et al. reported the successful hypothermic storage of neonatal rat ventricular CM monolayers for up to 72 hours in HTS. After this storage period, CMs retained their viability, metabolic activity (82% by day 1 after storage), and spontaneous contractile activity [16]; nevertheless, the impact of hypothermic storage on CM structure, ultrastructure, action potential, and drug responsiveness was not evaluated.

To date, there have been no studies reporting the efficient hypothermic storage of PSC-CMs. Therefore, in this study, we aimed to develop efficient strategies for hypothermic storage of murine and human PSC-CMs. The CM differentiation protocols are conventionally performed in two-dimensional (2D) monolayers or, more recently, in three-dimensional (3D) cell configurations, such as cell aggregates [7, 30]. It is well known that cell-cell and cell-matrix interactions play a critical role in cell survival/recovery after thawing [31]. Disruption of these interactions may result in dissociation-induced apoptosis [32]. Consequently, we evaluated the feasibility to cold-store CMs obtained from different PSC lines as 2D monolayers and 3D aggregates and assessed the impact of the hypothermic storage time on cell viability and metabolic activity recovery.

Cell phenotype, including structure, ultrastructure, gene and protein expression, and functionality, were assessed after storage by quantitative reverse-transcription polymerase chain reaction (RT-PCR), flow cytometry, fluorescent microscopy, scanning electron microscopy, transmission electron microscopy, and electrophysiology analyses.

MATERIALS AND METHODS

CM Differentiation of Murine PSCs

A murine transgenic α-PIG induced pluripotent stem cell (miPSC) line was used in this study. This cell line was genetically modified to integrate and stably express a transgene containing puromycin-N-acetyl transferase and enhanced green fluorescent protein (eGFP) genes, both under control of the cardiac-restricted promoter α-myosin heavy chain (α-MHC) [33]. miPSCs were expanded and differentiated as aggregates in fully controlled bioreactors as previously described by our group [8]. Briefly, iPSCs were inoculated in the WAVE Cellbag (GE Healthcare, Piscataway, NJ, http://www.gelifesciences.com) as single cells, at a concentration of 7×10^4 cell per ml, and were cultivated under defined conditions (temperature, 37°C; pO$_2$, 4% O$_2$; CO$_2$, 5%; surface aeration rate, 0.1 air volume per working volume per minute (vvm); rocking angle, 4°; agitation rate, 10–26 rpm; working volume, 1 liter) in differentiation medium (Iscove's modified Dulbecco's medium with GlutaMAX, supplemented with 20% [vol/vol] fetal bovine serum, 1% [vol/vol] nonessential amino acids, 1% [vol/vol] penicillin/streptomycin, and 50 μM β-mercaptoethanol [all from Invitrogen, Carlsbad, CA, http://www.invitrogen.com]). At day 9, cell lineage selection was induced by addition of puromycin (8 μg/ml). At day 11, cell aggregates composed of more than 97% of miPSC-CMs were harvested from Wave bioreactor. These cell aggregates were either preserved (as described in Hypothermic Storage of PSC-CMs) or dissociated into single cells by using 0.25% (wt/vol) trypsin/EDTA, and plated, at 5×10^5 cells per cm^2, in 24-well plates coated with CELLstart CTS [Invitrogen]). Cells were cultivated at 37°C, in a humidified atmosphere of 5% CO$_2$, until hypothermic storage studies were performed.

CM Differentiation of hPSCs

Two hPSC lines were used: hiPSC DF19-9-11T.H (WiCell, Madison, WI, http://www.wicell.org) and human embryonic stem cell (hESC) line NKX2-5(eGFP/w) [34] (kindly provided by Dr. David Elliott, Murdoch Children's Research Institute, Parkville, Victoria, Australia). HPSCs were cultured on Synthemax II SC Substrate-coated (Corning, Corning, NY, http://www.corning.com) plates in mTeSR1 (StemCell Technologies, Vancouver, BC, Canada, http://www.stemcell.com) medium until reaching 80% confluence. Cardiomyocyte differentiation was induced as described by Lian et al. [35]. By using this protocol, 2D monolayer cultures composed by 50%–70% of hPSC-CMs were obtained. To enrich the cell population into CMs, cells were cultured in CM enrichment medium (RPMI 1640 without glucose [Invitrogen] supplemented with B27 without insulin [Invitrogen] and 4 mM sodium L-lactate [Sigma-Aldrich, St. Louis, MO, http://www.sigmaaldrich.com]) for 10 days as described elsewhere [32]. After CM enrichment (more than 80% vascular cell adhesion molecule [VCAM]- and signal regulatory protein alpha [SIRPA]-positive cells), monolayer cultures were dissociated into single cells by incubation with TrypLE Select (Invitrogen) for 5 min. These cells were (a) replated at 5×10^5 cells per cm^2 in

Synthemax II SC Substrate-coated (Corning) 24-well plates and maintained for 1 week at 37°C in a humidified atmosphere of 5% CO_2, until hypothermic storage studies; and (b) aggregated as described in the literature [36]. Briefly, 5×10^5 cells were inoculated per well of low-adherent U-bottom 96-well plates (Nunc, Sigma-Aldrich, St. Louis, MO, http://www.sigmaaldrich.com), centrifuged at 500g for 5 min, and cultured in differentiation medium (RPMI 1640 [Invitrogen] supplemented with B27 without insulin) for 1 week until preservation tests.

Hypothermic Storage of PSC-CMs

The 2D monolayer cultures and 3D aggregates of murine and human PSC-CMs were stored at 4°C in HypoThermosol-FRS solution (BioLife Solutions, Bothell, WA, http://www.biolifesolutions.com) for 3, 5, and 7 days (designated as S3, S5, and S7, respectively). Immediately before hypothermic storage, culture medium was replaced by the following volumes of HTS solution: 2D monolayers, 300 μl per well in a 24-well plate; 3D aggregates, 150 μl per well in a 96-well plate (1 aggregate per well) or 1 ml per cryovial (300 aggregates per cryovial). After the hypothermic storage interval, HTS solution was removed, murine, and human PSC-CMs were washed once with the respective differentiation medium (described in CM Differentiation of Murine PSCs and CM Differentiation of hPSCs) and cultivated in the same medium for 7 days. In the first 24 hours after storage, medium was supplemented with 10 μM of RhoA kinase (ROCK) inhibitor (Y-27632; Biogen Cientifica SL, Madrid, Spain, http://www.biogen.es). Medium was totally exchanged at days 0, 1, 3, and 7 of culture. Methods for evaluation PSC-CM viability and metabolic activity and for assessment of PSC-CM phenotype and function, after cold storage, are provided in the supplemental online data.

RESULTS

Impact of Hypothermic Storage on PSC-CM Viability and Metabolic Activity

In this study, we aimed at developing a protocol for hypothermic storage of PSC-CMs, cultured either as 2D monolayers or 3D aggregates, to ensure efficient short-term preservation and/or shipping of PSC-CM suitable for clinical applications and toxicology testing. Murine and human PSC-CMs were preserved at hypothermic conditions (4°C) for 3, 5, and 7 days (designated hereafter as S3, S5, and S7, respectively), in HypoThermosol-FRS preservation solution. HTS was used because it is a xeno-free, cGMP, and clinically compatible solution that has been successfully used for hypothermic preservation of multiple cell types, including neonatal rat CMs [16].

Our results show that miPSC-CMs can be efficiently stored for 7 days in hypothermic conditions in HTS solution, without compromising cell viability or metabolic activity (supplemental online Fig. 1). Both 2D monolayers and 3D aggregates of iPSC-CMs remained highly viable after cold storage (supplemental online Fig. 1A) and maintained α-MHC driven eGFP expression (supplemental online Fig. 1A). By day 7 of culture after storage, both 2D monolayers and 3D aggregates of mPSC-CMs had nearly recovered their metabolic activity (>90%, as determined by the PrestoBlue assay; supplemental online Fig. 1B).

hPSC-CMs were more sensitive to hypothermia-induced stress than mPSC-CMs. Our results showed that high cell viabilities (80%) could be obtained when 2D monolayers of hPSC-CMs were preserved at hypothermic conditions for 3 days (S3 condition, Fig. 1A, 1B). However, cell viability after storage decreased

with increased cold-storage intervals (Fig. 1; Table 1). Specifically, cell viabilities, determined by the Trypan Blue exclusion method (Fig. 1A), and metabolic activity recoveries, evaluated by using the PrestoBlue assay (Fig. 1B; Table 1), of approximately 60% and 50% were estimated for S5 and S7 conditions, respectively. The marked propidium iodide (PI) and NucView Caspase-3 substrate staining (Fig. 1C) and the significantly higher cell lysis measured by the lactate dehydrogenase (LDH) activity in the supernatant (Fig. 1D) at day 1 after storage confirmed that cell death was more pronounced in the S7 condition. We verified that the caspase activity of stored hiPSC-CMs (immediately and 24 hours after cold storage) in the S7 condition increased in relation to the hiPSC-CMs before hypothermic storage (Fig. 1E). More specifically, we observed a significant increase in the activity of apoptotic initiator caspases (-8, -9, and -10) and apoptotic effector caspases (-3/7 and -6). The highest increase in caspase activity (approximately 1.7-fold increase) was registered in caspase 3/7, 24 hours after cells were removed from hypothermic storage, corroborating the pronounced NucView Caspase-3 substrate staining shown in Fig. 1C. All together, these results allowed us also to perceive that cell death occurred mainly from day 0 to 1 of culture after storage by both necrosis and apoptosis. Nonetheless, after 7 days in culture after storage, cells that recovered from hypothermia remained viable, adherent to culture dishes without meaningful PI/NucView staining (Fig. 1C). MitoView staining also highlighted the presence of abundant and functional mitochondria, a typical CM feature (Fig. 1C lower). It is worth noting that after all cold-storage intervals (S3, S5, and S7), cells restored their metabolism, as shown by similar values of specific glucose and glutamine consumption rates and lactate production rate when compared with the control, hiPSC-CMs not subjected to hypothermic storage, that is, maintained in culture during the storage period (Table 1).

Similar profiles of cell recovery were obtained when CMs derived from a hESC line were preserved as 2D monolayers (supplemental online Fig. 2). Specifically, cell recoveries of 80% were obtained after 5 days of hypothermic storage (supplemental online Fig. 2A, condition S5), but increased storage intervals (condition S7) led to a significant decrease in cell viability and metabolic activity recovery (42%, as determined by the PrestoBlue assay; Fig. 2A). After both storage intervals, cells that survived to hypothermic storage recovered their metabolism (supplemental online Fig. 2B).

Hypothermic preservation of hiPSC-CMs cultured as 3D aggregates led to higher cell recoveries than when cultured as 2D monolayers. From 3 days in culture after storage onward, no significant differences in metabolic activity recovery were detected between S5 and S7 conditions (Fig. 2B). By day 7 of culture after storage, metabolic activity recoveries of 66% and 71% were determined by the PrestoBlue assay in S5 and S7 conditions, respectively (Fig. 2B; Table 1). No necrotic centers were observed in aggregates from S5 and S7, and just a few PI-positive cells randomly distributed through the aggregate were detected at day 1 after storage (Fig. 2A). Importantly, contrary to what was observed in 2D monolayer cultures (Fig. 1E), after hypothermic storage of hiPSC-CM aggregates, the activity of initiator and effector caspases did not change significantly and was even lower for some stored samples in relation to hiPSC-CMs before hypothermic storage (Fig. 2C). These data indicate that when hiPSC-CMs are stored in this configuration, cell death by apoptosis is not meaningful.

In scanning electron microscopy images, it was possible to identify a higher amount of dead cells/cellular debris on the surface of the aggregates subjected to hypothermic storage
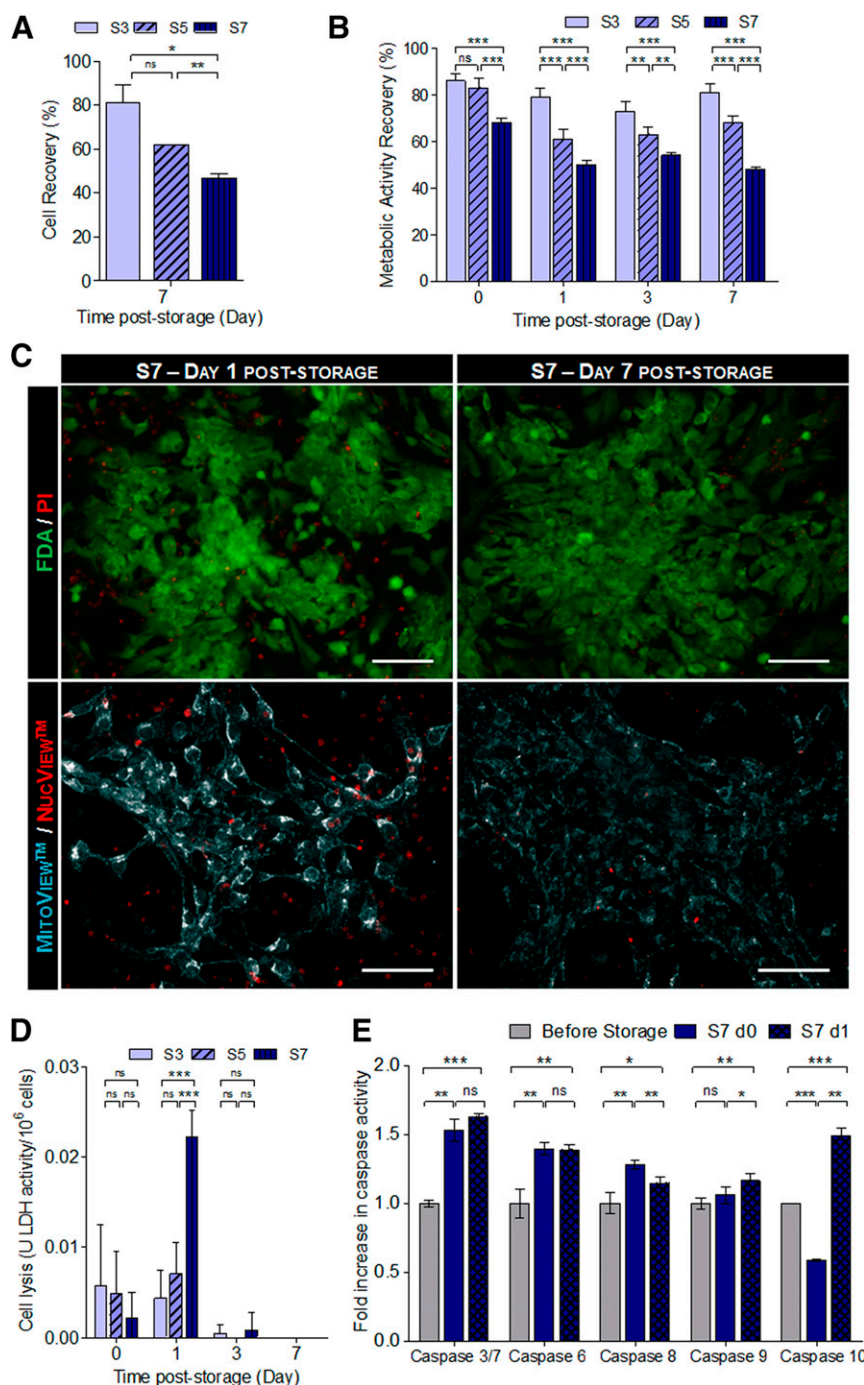
Figure 1. Hypothermic storage of hiPSC-CMs as two-dimensional monolayers. hiPSC-CMs were stored for 3, 5, and 7 days at 4°C in HypoThermosol solution. Cell recovery was evaluated for 7 days after storage. **(A):** Evaluation of cell recovery after the storage interval and 7 days of culture using the Trypan Blue exclusion method. **(B):** Assessment of metabolic activity recovery using the PrestoBlue assay. The cell concentration **(A)** and the fluorescence values of PrestoBlue **(B)** are presented as a percentage in relation to the values obtained in the cells immediately before cold storage. **(C):** Upper panel: Viability analysis of hiPSC-CMs from the S7 condition, assessed at days 1 and 7 after storage, using the FDA (live cells; green) and PI (dead cells; red). Lower panel: Detection of caspase-3 activity using NucView Caspase-3 Substrate (red) and the MitoView mitochondrial dye (cyan) at days 1 and 7 after storage in S7 cultures. Scale bars = 100 μm. **(D):** Cell lysis measured by the LDH activity in the culture supernatant. Values are normalized by the number of cells. **(E):** Fold increase in the activity of caspases-3/7, -6, -8, -9, and -10 immediately and 24 hours after hypothermic storage in the S7 condition in relation to the cells before storage. Data are presented as mean ± SD of three **(A)**, four **(E)**, and five **(B, D)** measurements. ∗, $p < .05$; ∗∗, $p < .01$; ∗∗∗, $p < .001$, determined by one-way analysis of variance and unpaired t test. Abbreviations: d0, 0 days after storage; d1, 1 day after storage; FDA, fluorescein diacetate; hiPSC-CM, human induced pluripotent stem cell-derived cardiomyocyte; LDH, lactate dehydrogenase; ns, not significant; PI, propidium iodide; S3, stored for 3 days; S5, stored for 5 days; S7, stored for 7 days.

Table 1. Evaluation of hiPSC-CM recovery after 3, 5, and 7 days of storage at 4°C in HypoThermosol preservation solution

	2D monolayers				3D aggregates		
	S3	S5	S7	Control	S5	S7	Control
Metabolic activity recovery (%)							
Day 1 poststorage	79 ± 5	61 ± 5	50 ± 3	—	92 ± 15	80 ± 14	92 ± 12
Day 7 poststorage	81 ± 4	68 ± 3	48 ± 2	—	63 ± 17	70 ± 18	86 ± 11
qMet (mmol·10^{-9}cells·hour^{-1})							
qGLN	0.03 ± 0.01[a]	0.02 ± 0.00[b]	0.02 ± 0.00[a]	0.01 ± 0.00	0.03 ± 0.00, NS	0.02 ± 0.01, NS	0.02 ± 0.00
qGLC	0.08 ± 0.01, NS	0.09 ± 0.01, NS	0.07 ± 0.01, NS	0.08 ± 0.01	0.10 ± 0.02, NS	0.11 ± 0.04, NS	0.09 ± 0.03
qLAC	0.13 ± 0.01, NS	0.11 ± 0.02, NS	0.09 ± 0.01, NS	0.13 ± 0.01	0.15 ± 0.02, NS	0.14 ± 0.02, NS	0.17 ± 0.03

Values denote the mean ± SD of 5 (2D monolayers) and 15 (3D aggregates) measurements. Significant differences in relation to the control (cells not subjected to hypothermic storage maintained under conventional culture conditions for 14 days [i.e., equivalent to 7 days of storage plus 7 days of poststorage recovery]) were determined by an unpaired t test with Welch's correction.
[a]$p < .001$.
[b]$p < .01$.
Abbreviations: —, no data; 2D, two-dimensional; 3D, three-dimensional; hiPSC-CM, human induced pluripotent stem cell-derived cardiomyocyte; NS, not significant; qGLC, specific consumption rate of glucose; qGLN, specific consumption rate of glutamine; qLAC, specific production rate of lactate; qMet, specific consumption/production rate of metabolites; S3, stored for 3 days; S5, stored for 5 days; S7, stored for 7 days.

comparatively to control aggregates (hiPSC-CM aggregates not subjected to cold storage; Fig. 2D vs. Fig. 2E). These results were also confirmed by PrestoBlue assay because lower cell viabilities and metabolic activities after storage were attained in S5 and S7 conditions comparatively to the control (Fig. 2B). Noteworthy, after 7 days of culture after storage, aggregates from S7 condition maintained their structure, being almost indistinguishable from control aggregates (Fig. 2D vs. Fig. 2E). In accordance, no significant differences ($p > .05$) in aggregate size were detected between aggregates from the S7 condition (269 ± 17 μm; Fig. 2D) and control aggregates (256 ± 13 μm; Fig. 2E). The metabolic profile, namely, specific glucose and glutamine consumption rates and lactate production rate, was also not significantly different from control aggregates (Table 1).

Effect of Hypothermic Storage on PSC-CM Phenotype

Hypothermic storage may affect not only cell viability and metabolic activity, but also cell phenotype and function [37]. Although we showed that hPSC-CMs are more resistant to prolonged hypothermic storage-induced cell injury in 3D aggregates than in 2D monolayers, we intended to confirm also that viable cells recovered after hypothermic storage in 2D monolayers maintain their phenotype. Thus, we assessed the effect of hypothermic storage on the structure and functional features of hPSC-CMs storage as 2D monolayers and 3D aggregates. Our results showed that PSC-CMs, stored either as 2D monolayers or 3D aggregates, recovered from all hypothermic storage intervals (S3, S5, and S7), restored their metabolism (Table 1), retained the expression of cardiac markers (determined by flow cytometry; Figs. 3A and 4A), and the contractile function (Figs. 3B and 4B). Therefore, cells subjected to a longer period of hypothermic storage (S7 condition) were selected and further characterized in terms of gene expression, cell structure, ultrastructure, and function.

Quantitative RT-PCR analysis was performed for hiPSC-CMs stored as 2D monolayers. The results revealed that, after 7 days in culture after storage, CM-specific genes, with the exception of VCAM1, and the cardiac progenitor-related genes, KDR and GATA4, were highly expressed in hPSC-CMs subjected to cold storage than in the control (i.e., nonstored cells that were maintained in culture for 14 days, which corresponds to the 7 days of

hypothermic storage plus 7 days in culture after storage) (Fig. 3B). These data suggest a hypothetical role of hypothermia in CM enrichment and/or maturation (cardiac progenitor cells present in culture before hypothermia might be more sensitive to cold storage-induced stresses than CMs with a more mature phenotype).

To access morphology and structure of hiPSC-CMs stored as 3D aggregates, immunofluorescence microscopy analysis was carried out. Our results showed that hiPSC-CMs exhibited a typical cardiac morphology, with highly organized sarcomeric α-actinin, titin, troponin I, and troponin T after 7 days of hypothermic storage (Fig. 4C). Similar results were attained for miPSC-CMs that also expressed Myl2, Myl7, and α-MHC (supplemental online Fig. 3), as well as for cells stored as 2D monolayers (not shown).

Transmission electron microscopy analysis revealed that after the storage interval and 7 days in culture after storage, hiPSC-CMs cultured either as 2D monolayers (Fig. 5A) or 3D aggregates (Fig. 5B) did not display signals of microstructural damage (such as damaged cell membranes and organelles) and showed ultrastructural features indistinguishable from the hiPSC-CMs not subjected to hypothermic storage (control; Fig. 5C). Myofilaments organized in myofibrils with a sarcomeric pattern were observed, as well as abundant long and slender mitochondria. Z bands delimiting the sarcomeres and highly specialized cell-cell junctions (intercalated disks) were also identified in both culture configurations (Fig. 5A, 5B). No other bands were visible in the sarcomere construct, in the cold-stored hiPSC-CMs and control (Fig. 5A–5C). The aligned sarcomeres in stored hiPSC-CMs presented a mean length of 1.40 ± 0.06 μm, similar to the control (1.49 ± 0.09 μm) and to sarcomere length reported in literature for early and immature hiPSC-CMs (1.50 ± 0.15 μm) [38].

Characterization of hiPSC-CM Function After Hypothermic Storage

We verified that after all storage intervals, murine (not shown) and human iPSC-CMs stored as 2D monolayers and 3D aggregates regained their normal beating frequency after 3–4 days in culture (Fig. 3B, supplemental online Fig. 3B, and supplemental online
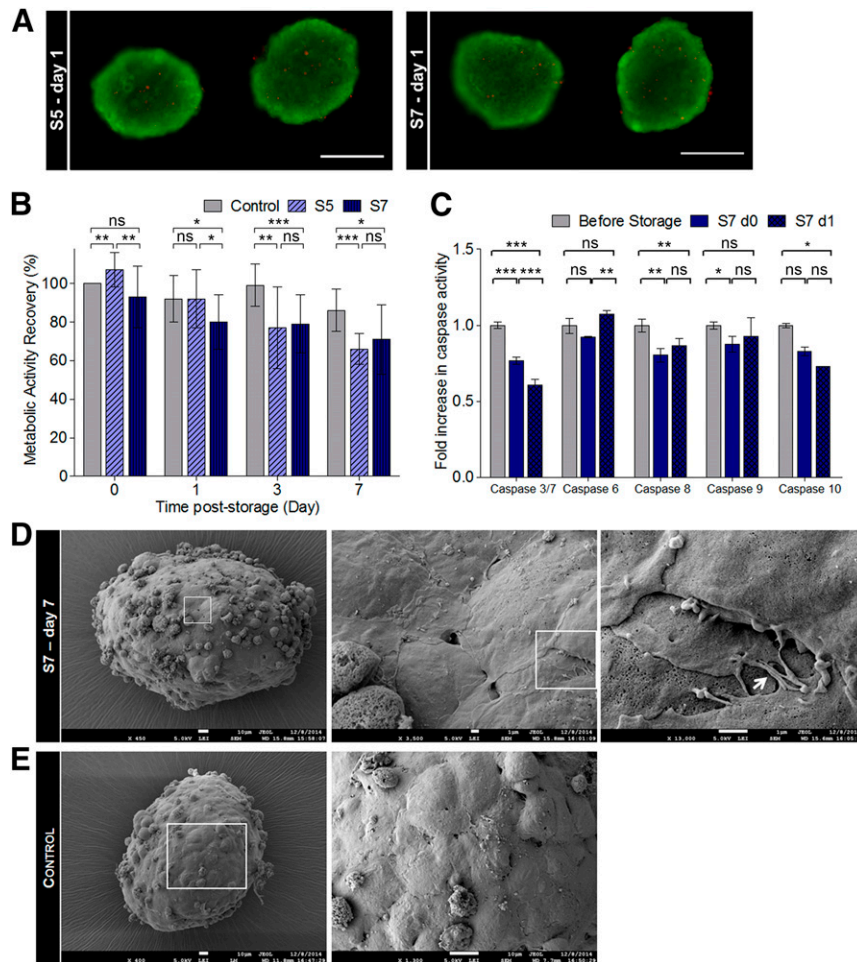
Figure 2. Hypothermic storage of hiPSC-CMs as three-dimensional aggregates. Aggregates were stored for 5 and 7 days at 4°C in HypoThermosol solution. Cell recovery was evaluated for 7 days after storage. **(A):** Cell viability at day 1 after storage assessed by using fluorescein diacetate (live cells; green) and propidium iodide (dead cells; red) dyes. **(B):** Evaluation of metabolic activity recovery after storage by PrestoBlue assay. The fluorescence values are presented as a percentage in relation to the values obtained in the cells immediately before cold storage. **(C):** Fold increase in the activity of caspases-3/7, -6, -8, -9, and -10 immediately and 24 hours after hypothermic storage in S7 condition in relation to the cells before storage. **(D, E):** Scanning electron microscopy of hiPSC-CM aggregates from S7 condition after 7 days in culture after storage **(D)** and the control (hiPSC-CM aggregates not subjected to cold storage, i.e., maintained in culture during the storage period) **(E)**. The boxed regions were magnified to show cell boundaries and cell-cell contacts (arrow). Scale bars = 200 μm **(B)**, 10 μm **(C left, D)**, and 1 μm **(C middle and right)**. Data are presented as mean ± SD of 4 **(C)** and 15 **(B)** measurements. *, $p < .05$; **, $p < .01$; ***, $p < .001$; ns as determined by unpaired t test. Abbreviations: d0, 0 days after storage; d1, 1 day after storage; hiPSC-CM, human induced pluripotent stem cell-derived cardiomyocyte; ns, not significant; S5, stored for 5 days; S7, stored for 7 days.

Movie 1). The action potential (AP) characteristics of miPSC-CMs cold-stored as 2D monolayers were very similar to control miPSC-CMs, showing comparable maximum diastolic potential, beating frequency, velocity of diastolic depolarization, AP upstroke velocity, and AP duration (supplemental online Fig. 4A). Moreover, the response of cold-stored and control miPSC-CMs to cardiostimulatory drugs was not significantly different. When the adrenergic agonist isoproterenol was administered, a similar increase of AP frequency was observed (supplemental online Fig. 4B). Positive chronotropic effects of isoproterenol were reversible upon washout (supplemental online Fig. 4B).

Characterization of hiPSC-CM function after 7 days of hypothermic storage as 2D monolayers plus 7 days in culture was assessed by recording inward and outward whole-cell K$^+$ conductances in voltage-clamp experiments using the whole-cell patch-clamp configuration. After obtaining "whole-cell mode," brief measurements of membrane potential (V_m, under current clamp) were conducted

before shifting to voltage clamp. These recordings revealed that cell membranes were adequately polarized after 7 days of cold storage ($V_m = -69.2 \pm 0.6$ mV; $n = 8$). To evaluate voltage dependence of transmembrane currents, a wide range of potentials was used to record currents following 10 mV steps (of 260 ms) from -130 to $+0$ mV, while keeping the holding potential at -70 mV (Fig. 6A left). The corresponding curves revealed three main components: (a) a clear inward component from -130 to -60 mV (component that may correspond to the typical cardiac inward K rectifier, I$_{kr}$); (b) an inward "hump" from -50 to -20 mV; and (c) a typical delayed outward K$^+$ current above -10 mV (Fig. 6A right). To investigate the outward K$^+$ current, a less abrasive single voltage step (to $+40$ mV) was performed (Fig. 6B). This protocol consisted in a brief depolarization (50 ms) to -10 mV aiming at Ca^{2+} influx through voltage-activated channels, which was immediately followed by a longer depolarizing step (750 ms) to $+40$ mV.
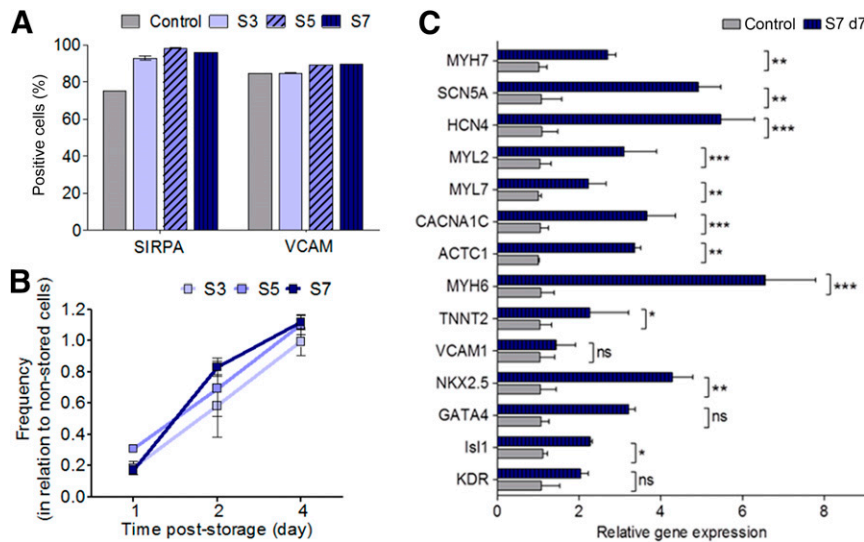
Figure 3. Characterization of hiPSC-CMs stored as two-dimensional (2D) monolayers in hypothermic conditions for up to 7 days. **(A):** Percentage of SIRPA and VCAM-positive cells determined by flow cytometry. **(B):** The beating frequency (beats per minute) after all storage intervals (S3, S5, and S7) was monitored until day 4 of culture after storage in hiPSC-CMs cultured as 2D monolayers. The results were normalized to the beating frequency measured in the control cells not subjected to cold storage. **(C):** Quantitative reverse-transcriptase polymerase chain reaction analysis showing the relative expression of cardiac-related transcription factors, cardiac-specific structural genes, calcium handling, and membrane ion channels in the S7 condition, after 7 days in culture poststorage. Values were normalized to the control, cells not subjected to cold storage, and maintained in culture for the same time period. Data are presented as mean $\pm$ SD of at least three measurements. $*$, $p < .05$; $**$, $p < .01$; $***$, $p < .001$; ns, as determined by unpaired t test. Abbreviations: d7, after 7 days in culture poststorage; hiPSC-CM, human induced pluripotent stem cell-derived cardiomyocyte; ns, not significant; SIRPA, signal-regulatory protein alpha; VCAM, vascular cell adhesion molecule.
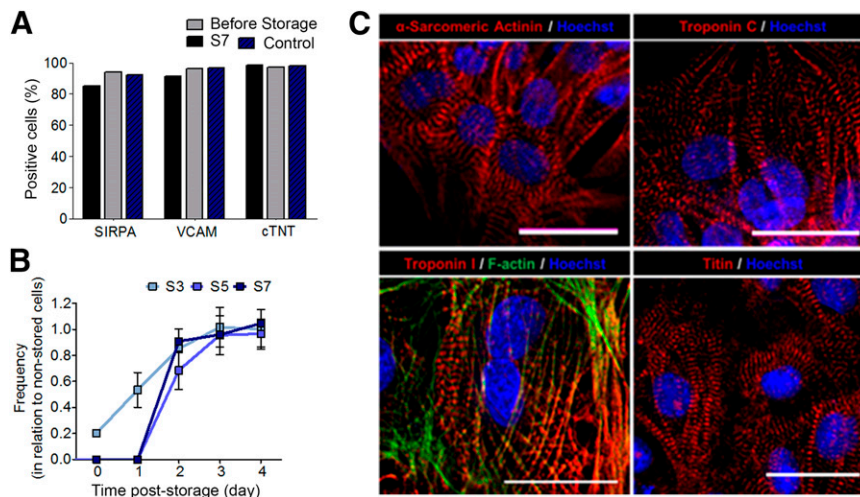

Figure 4. Characterization of hiPSC-CMs stored as three-dimensional (3D) aggregates in hypothermic conditions for up to 7 days. **(A, C):** After hypothermic storage and 1 week in culture after storage, cells were characterized by flow cytometry **(A)** and immunofluorescence staining **(C)** for cardiac-specific markers. **(B):** The regained of contractile activity was also assessed by phase-contrast microscopy. **(A):** Percentage of SIRPA, VCAM, and cTNT-positive cells determined by flow cytometry. **(B):** The beating frequency (beats per minute) after all storage intervals (S3, S5, and S7) was monitored until day 4 of culture after storage. The results were normalized to the beating frequency measured in the control cells not subjected to cold storage. **(C):** Immunofluorescence analysis of hiPSC-CMs (from plated 3D aggregates) after hypothermic storage for the CM-specific markers: sarcomeric α-actinin, Troponin C, Troponin I, and Titin (red) antibodies. F-actin is stained with phalloidin (green). Nuclei were counterstained with Hoechst (blue). Scale bars = 30 μm. Abbreviations: cTNT, cardiac troponin T; hiPSC-CM, human induced pluripotent stem cell-derived cardiomyocyte; S3, stored for 3 days; S5, stored for 5 days; S7, stored for 7 days. SIRPA, signal-regulatory protein alpha; VCAM, vascular cell adhesion molecule.

The inward current hump detected in the current-voltage relationship between -50 and 0 mV (Fig. 6A) suggests the activation of voltage-gated calcium channels, allowing Ca^{2+} influx mainly through Ca$_V$1 (L-type) channels [39]. Even though we did not perform experiments to directly evaluate calcium dynamics, it is likely that activation of voltage-activated calcium channels may account for the inward current hump observed here. Thus, Ca^{2+} recruitment through voltage-gated channels, most probably via Ca$_V$1 (L-type) channels, ensures that coupling to small-conductance Ca^{2+}-activated K$^+$ outward currents occur as
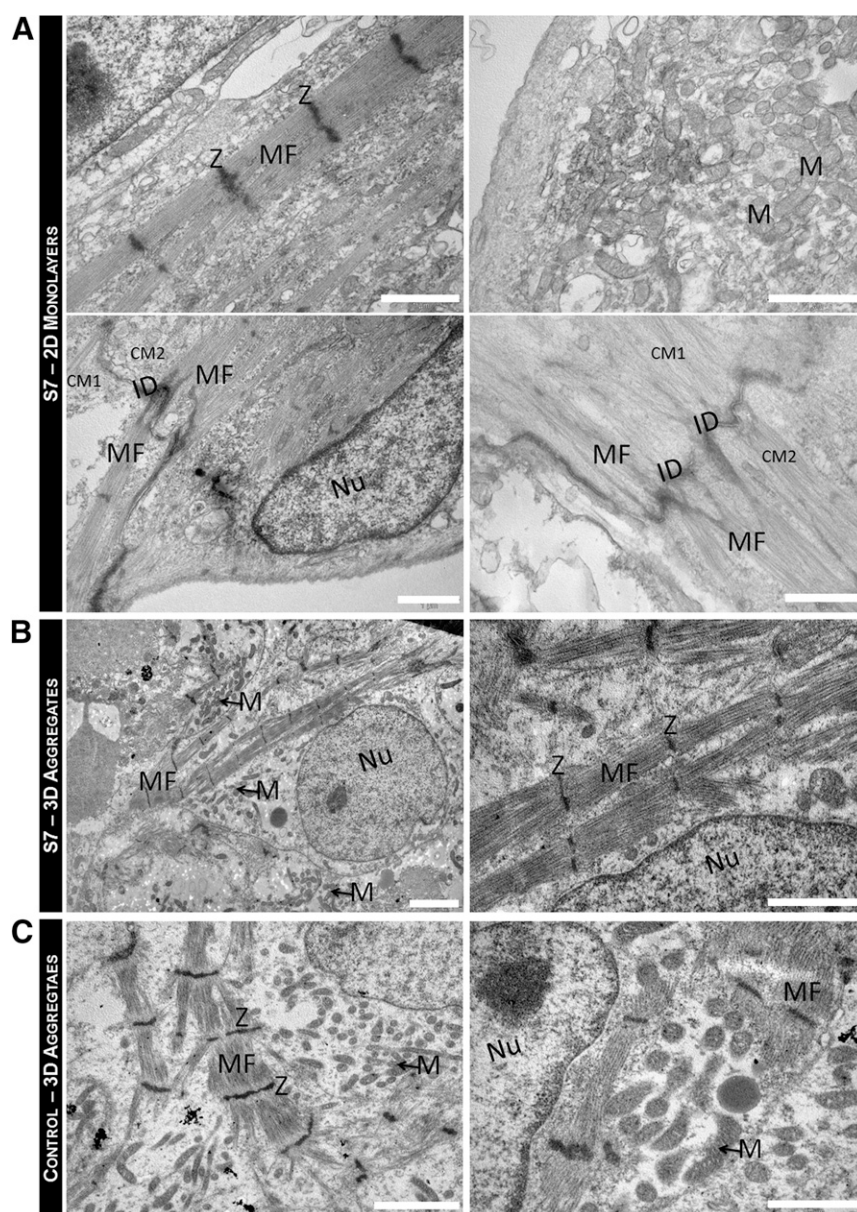
Figure 5. Ultrastructural characterization of hiPSC-CMs after hypothermic preservation. **(A, B):** Transmission electron microscopy (TEM) images of hiPSC-CMs, stored at hypothermic conditions for 7 days, as 2D monolayers **(A)** and as 3D aggregates **(B)**. **(C):** TEM images of the control 3D aggregates: hiPSC-CMs not subjected to hypothermic storage, that is, maintained in culture during the storage period (control). HiPSC-CMs presented a large nucleus (Nu)-to-cytoplasm ratio and contained many myofibrils aligned and organized in a sarcomeric pattern. Z-bands and neighboring CMs (CM1 and CM2) connected by intercalated disks were also observed. Scale bars = 1 μm **(A, B** right**, C** right**)** and 2 μm **(B** left**, C** left**)**. Abbreviations: 2D, two-dimensional; 3D, three-dimensional; CM, cardiomyocyte; hiPSC-CM, human induced pluripotent stem cell-derived cardiomyocyte; ID, intercalated disks; M, mitochondria; MF, myofibrils; Nu, nucleus; S7, stored at hypothermic conditions for 7 days; Z, Z-band.

described for CMs [40]. Consistent with this, we showed that the outward K$^+$ current (Fig. 6B) was clearly voltage-dependent, with the maximal amplitude obtained when cells were depolarized with a prepulse reaching −10 mV—that is, close to the maximum activation of Ca$_V$1 (L-type) currents.

Indirect measurements of contractions obtained from video data analysis revealed that hiPSC-CMs subjected to 7 days of cold storage as 2D monolayers respond appropriately to different chronotropic agents (Fig. 6C–6H). An increase in K$^+$ concentration from 5 to 30 mM shifted the potential equilibrium of K$^+$, resulting in membrane potential depolarization and, consequently, in a

strong and sustained contraction (Fig. 6C). The addition of verapamil (1 μM), which specifically blocks L-type Ca^{2+} channels, reduced the beating frequency and ultimately arrested beating (Fig. 6D). Conversely, the administration of 0.5 μM adrenaline, a β-receptor agonist, significantly increased the beating frequency of hiPSC-CMs, but not the duration of the contraction events (Fig. 6E, 6F). The treatment with nimodipine (300 pM), a L-type Ca^{2+} channel blocker, evoked subtle but meaningful effects on beating behavior. Beating frequency remained constant, whereas the duration of the contractions significantly decreased (Fig. 6G, 6H). These data strongly suggested the existence of
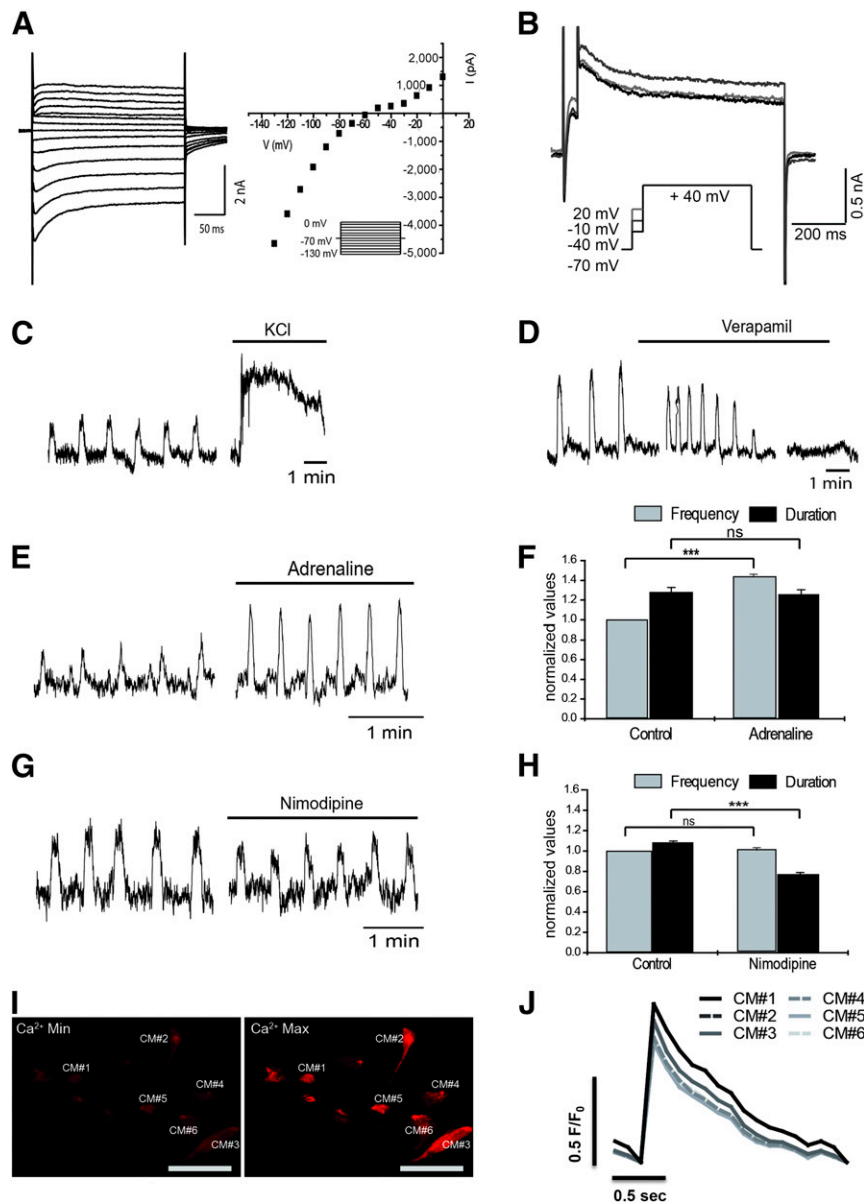
Figure 6. Functional characterization of hiPSC-CMs subjected to hypothermic storage for 7 days. After hypothermic storage for 7 days and 1 week in culture after storage, cell functionality was evaluated by the detection of CM-specific action potentials (AP) **(A, B)**, typical CM response to drugs **(C–H)**, and calcium transients **(I, J)**. **(A):** Whole-cell voltage-clamp recordings from hiPSC-CMs subjected to 7 days of hypothermic storage as 2D monolayers. **(A):** Left: Representative currents following a set of voltage pulses (260 ms), covering a wide range of potentials, with incremental depolarization steps (10 mV) from −130 to 0 mV (holding voltage −70 mV) (inset). Right: Corresponding current-voltage relationship showing three different components in terms of voltage dependence: a strong inward rectifier, an inward hump, and a delayed outward current. **(B):** Representative current traces from a triple set of double depolarizing pulses: one first step to −40, −10, and +20 mV, lasting 50 ms, followed by a second pulse to +40 mV, lasting 750 ms (inset). One can notice a larger outward current at +40 mV when preceded by a prepulse to −10 mV, which suggest a Ca^{2+}-dependent current component. **(C–H):** Effect of chronotropic drugs: 30 mM KCL **(C)**, 1 μM Verapamil **(D)**, 0.5 mM Adrenaline **(E, F)**, and 300 pM Nimodipine **(G, H)**, on contractile activity of hiPSC-CMs (cultured as 2D monolayers) subjected to 7 days of hypothermic storage, analyzed by video recording in an inverted microscopy. **(I):** Pseudocolor images showing minimal (Ca^{2+} min; left) and maximal (Ca^{2+} max; right) intensity of the calcium indicator dye Rhod-3. The six hiPSC-CMs analyzed (from plated 3D aggregates) are highlighted. **(J):** Graphical representation of calcium level cycling, during hiPSC-CMs contraction, determined by confocal imaging of the Rhod-3 dye, for the six different hiPSC-CMs. Data are presented as mean ± SD of 24 **(F, H)** measurements. ∗∗∗, $p < .001$; ns, as determined by unpaired *t* test. Abbreviations: CM, cardiomyocyte; hiPSC-CM, human induced pluripotent stem cell-derived cardiomyocyte; Max, maximal; Min, minimal; ns, not significant.

L-type voltage-activated Ca^{2+} currents in hiPSC-CMs after hypothermic storage.

Real-time intracellular calcium imaging, using the calcium indicator dye Rhod-3, revealed that 2D monolayers (not shown) and

3D aggregates of hiPSC-CMs present synchronized oscillatory patterns of intracellular calcium concentrations (Fig. 6I, 6J). Supplemental online Movie 2 shows a representative live imaging recording of whole-cell calcium transients of iPSC-CMs after cold

storage. Overall, these results clearly show that murine and human iPSC-CMs exhibit intact molecular, ultrastructural, and functional properties after 1 week of hypothermic storage.

DISCUSSION

Several studies have focused on the development of methods to preserve primary cultures of neonatal and adult CMs from rat and mouse origin [16, 41–45], but little has been done to optimize the short- and long-term storage of hPSC-CMs that more accurately reflect the physiology of human CMs. In this study, we developed efficient strategies for the hypothermic storage of 2D monolayers and 3D aggregates of hPSC-CMs. We showed that both 2D cell monolayers and 3D cell aggregates of mPSC-CMs can be maintained for up to 1 week in hypothermic conditions without meaningful effects on cell viability (>90% of cell recovery), structure, and functionality (including action potential and drug responsiveness). However, we verified that hPSC-CMs are more sensitive to hypothermia/rewarming-induced stress than mPSC-CMs. A 30% decrease in cell viability was observed in hPSC-CMs preserved as monolayers, when the storage interval was extended from 3 to 7 days. In fact, it is not surprising that murine and human PSC-CMs present such a different tolerance to hypothermic storage because several studies have described significant differences in the transcriptional networks, global molecular signatures, and signaling pathways in mouse and human PSCs [46, 47]. These differences likely justify the distinct developmental potentials, culture requirements, and epigenetic landscapes observed in these cells [46]. Mu et al. showed significant differences in the induction of differentiation of murine and human ESCs into CMs, as well as in specific features of each CM derivative, including average beating frequency and response to 24 hours of hypoxia stimulation [48].

In this work, we showed that hPSC-CM aggregates subjected to 5 and 7 days of hypothermic preservation present similar cell recoveries after storage. After 7 days of hypothermic storage, cell recoveries were higher in PSC-CM aggregates (70%) than in PSC-CM monolayers (50%). These results suggest that a 3D architecture confers an additional protection to extended hypothermia-induced stress, possibly because of the formation of vast and stable cell-to-cell and cell-to-extracellular matrix (ECM) interactions. It has been reported that a tridimensional organization favors the establishment and maintenance of cellular junctions between cardiac cells [49]. In the same study, the authors demonstrated that aggregates of cardiac cells exhibit a larger number of intercellular junctions and a higher amount of ECM connecting the cells compared to 2D cultures [49]. Interestingly, it has been shown that in 3D conformations, cell extensions become entangled with ECM fibrils, resulting in integrin-independent mechanical interactions that strengthen cell anchorage [50]. All these findings support our supposition that spatial organization of PSC-CMs may affect their biological response to hypothermic storage.

It has been reported that hypothermic storage may induce adverse effects on cells, including hypoxic stress, ischemia and reperfusion injury, disruptions in membrane potential (redox balance), cellular ionic imbalances (disturbance of Na^+, Ca^{2+}, and Fe^{2+} homeostasis), generation of reactive oxygen species, collapse of cytoskeleton, and ultrastructural damage [37, 51–55]. These effects are more pronounced with increasing hypothermic storage intervals, resulting in the activation of necrotic or apoptotic cell death pathways [37, 55]. Activation of the apoptotic cascade takes hours to days to be fully manifested after cells or tissues

are removed from storage. Thus, to assess the efficiency of the preservation strategy, cell recovery should be assessed for an extended time period in culture after storage and preferably by using complementary characterization techniques. In this study, we evaluated CM recovery during 7 days of culture after storage, through the analysis of cellular membrane integrity (fluorescein diacetate/PI staining and Trypan Blue exclusion test), metabolic activity (PrestoBlue assay), and detection of apoptosis activation and mitochondrial activity (quantification of caspase activity and MitoView/NucView staining). As expected, extended hypothermic preservation intervals induced both necrosis and apoptosis of hPSC-CMs, particularly in 2D monolayer cultures. Nonetheless, hPSC-CMs that recovered from hypothermic storage, either in 3D aggregate or in 2D monolayer cultures, maintained their phenotype as reflected by a typical CM structure/ultrastructure and cardiac protein expression profile. The expression of typical CM genes (including transcription factors, specific structural genes, and ionic channels) were revealed to be significantly higher in stored hiPSC-CMs than in the control, suggesting that the hypothermia state may enhance CM enrichment/maturation processes. A recent study reported that apoptotic stimuli—more specifically, a sublethal caspase-activation—up-regulates cardiac progenitor and CM differentiation, increasing the final yield of CMs [56]. As shown in our study and in others [16, 37, 57], the hypothermic state promotes caspase activation; consequently, we could also speculate about an interference of cold preservation in cardiogenic pathways. Importantly, hiPSC-CMs subjected to 7 days of hypothermic storage maintained their functionality, exhibiting features typical form healthy CMs, including (a) several ionic conductances (IKr, outward delayed rectifiers, and Ca^{2+}-activated K^+ currents) [58], (b) indirect "fingerprints" of voltage-activated L-type Ca^{2+} currents [58], and (c) appropriate contractile activity response to chronotropic agents [59].

Commercially available hypothermic solutions, such as HTS, were carefully formulated to maintain the ionic and osmotic balances, inhibit acidosis, and prevent cell swelling at low temperatures [15, 37]. These features facilitate preservation of cell homeostasis, which is not achievable when using just culture medium as a preservation formulation. For example, normal human epidermal keratinocytes can be maintained for periods exceeding 1 week at 4°C in HTS and only 24 hours in normal growth medium at 4°C [21]. Currently, the incorporation of protective agents, including antioxidants, ion chelators, and membrane stabilizers, in preservation media has been reported to markedly improve preservation efficacy. For example, fructose-1,6-bisphosphate [42, 60], 2,3-butanedione [42, 61], myosin II ATPase inhibiting-agents [29], dopamine and lipophilic derivatives [45], and human neuregulin-1 peptide [62] proved to be efficient in improving the poststorage viability in mouse/rat hearts and/or CMs. A recent study with preserved bioartificial livers showed that an improved protective effect can be obtained if distinct agents are added to the storage solution during the appropriate preservation stage (preincubation, hypothermia, and rewarming) [63]. Specific protective agents could also be combined with our cold-storage preservation protocol to further enhance preservation efficacy after extended storage intervals.

CONCLUSION

We established effective and clinically compatible strategies for cold storage of 2D monolayers and 3D aggregates of murine and human PSC-CMs and provided some evidence about the

appropriate time interval to store PSC-CMs at hypothermic conditions without compromising their viability, phenotype, and function. These preservation strategies can be integrated with the differentiation process, avoiding additional and possible harmful manipulation of cells, such as monolayer/aggregate dissociation. Moreover, these strategies enable cell products to be manufactured off-site in certified companies. Importantly, our approach for hypothermic storage of 2D monolayers of PSC-CMs will facilitate the delivery of certified, validated, ready-to-use cell plates suitable for high-throughput cardiac drug testing and toxicity screening, whereas the 1-week storage strategy for PSC-CM aggregates will allow the distribution of not only off-the-shelf tissue like in vitro models for cardiac toxicity drug testing, but also therapeutic cells that could be directly used in cardiac regenerative therapies. In fact, it has been demonstrated that the delivery of cardiac progenitor cells in the form of 3D cell aggregates improved in vivo survival of implanted cells in a murine model of cardiac injury [64]. The strategies for cold preservation of PSC-CMs described herein contribute to overcoming the hurdles and needs of the regenerative medicine market and scientific community, constituting a step forward toward improved worldwide commercial distribution of hPSC-CMs for use in the clinic and biopharmaceutical industry.

AUTHOR CONTRIBUTIONS

C.C.: conception and design, collection and/or assembly of data, data analysis and interpretation, manuscript writing; A.K. and N.E.: collection and/or assembly of data, data analysis and interpretation; M.C. and P.A.L.: collection and/or assembly of data, data analysis and interpretation, manuscript writing; T.S.: provision of study material, manuscript writing; M.S. and P.M.A.: conception and design, manuscript writing, final approval of manuscript.

DISCLOSURE OF POTENTIAL CONFLICTS OF INTEREST

The authors indicated no potential conflicts of interest.

REFERENCES

1 Sinnecker D, Laugwitz K-L, Moretti A. Induced pluripotent stem cell-derived cardiomyocytes for drug development and toxicity testing. Pharmacol Ther 2014;143:246–252.

2 Lundy SD, Gantz JA, Pagan CM et al. Pluripotent stem cell derived cardiomyocytes for cardiac repair. Curr Treat Options Cardiovasc Med 2014;16:319.

3 Wang Y, Cheng L, Gerecht S. Efficient and scalable expansion of human pluripotent stem cells under clinically compliant settings: A view in 2013. Ann Biomed Eng 2014;42:1357–1372.

4 Chen KG, Mallon BS, McKay RDG et al. Human pluripotent stem cell culture: considerations for maintenance, expansion, and therapeutics. Cell Stem Cell 2014;14:13–26.

5 Serra M, Brito C, Sousa MFQ et al. Improving expansion of pluripotent human embryonic stem cells in perfused bioreactors through oxygen control. J Biotechnol 2010;148:208–215.

6 Serra M, Brito C, Correia C et al. Process engineering of human pluripotent stem cells for clinical application. Trends Biotechnol 2012;30:350–359.

7 Mummery CL, Zhang J, Ng ES et al. Differentiation of human embryonic stem cells and induced pluripotent stem cells to cardiomyocytes: A methods overview. Circ Res 2012;111:344–358.

8 Correia C, Serra M, Espinha N et al. Combining hypoxia and bioreactor hydrodynamics boosts induced pluripotent stem cell differentiation towards cardiomyocytes. Stem Cell Rev 2014;10:786–801.

9 Healy L, Young L, Stacey GN. Stem cell banks: preserving cell lines, maintaining genetic integrity, and advancing research. Methods Mol Biol 2011;767:15–27.

10 Abbasalizadeh S, Baharvand H. Technological progress and challenges towards cGMP manufacturing of human pluripotent stem cells based therapeutic products for allogeneic and autologous cell therapies. Biotechnol Adv 2013;31:1600–1623.

11 Li Y, Ma T. Bioprocessing of cryopreservation for large-scale banking of human pluripotent stem cells. Biores Open Access 2012;1:205–214.

12 Thirumala S, Goebel WS, Woods EJ. Clinical grade adult stem cell banking. Organogenesis 2009;5:143–154.

13 Rubinsky B. Principles of low temperature cell preservation. Heart Fail Rev 2003;8:277–284.

14 Baust JM. Advances in media for cryopreservation and hypothermic storage. Bioprocess Biosyst Eng 2005;(suppl):46–56.

15 Mathew AJ, Baust JM, Van Buskirk RG et al. Cell preservation in reparative and regenerative medicine: evolution of individualized solution composition. Tissue Eng 2004;10:1662–1671.

16 Snyder KK, Baust JM, Van Buskirk RG et al. Enhanced hypothermic storage of neonatal cardiomyocytes. Cell Preserv Technol 2005;3:61–74.

17 Mathew AJ, Van Buskirk RG, Baust JG. Improved hypothermic preservation of human renal cells through suppression of both apoptosis and necrosis. Cell Preserv Technol 2002;1:239–253.

18 Duret C, Moreno D, Balasiddaiah A et al. Cold preservation of human adult hepatocytes for liver cell therapy. Cell Transplant 2015;24:2541–2555.

19 Gramignoli R, Dorko K, Tahan V et al. Hypothermic storage of human hepatocytes for transplantation. Cell Transplant 2014;23:1143–1151.

20 Bessems M, Doorschodt BM, van Vliet AK et al. Preservation of rat livers by cold storage: A comparison between the University of Wisconsin solution and Hypothermosol. Ann Transplant 2004;9:35–37.

21 Cook JR, Eichelberger H, Robert S et al. Cold-storage of synthetic human epidermis in HypoThermosol. Tissue Eng 1995;1:361–377.

22 Hrabalová M, Bachleda P, Lubuská L et al. Effect of various protective solutions on function after kidney transplantation. Biomed Pap Med Fac Univ Palacky Olomouc Czech Repub 2003;147:197–202.

23 Squifflet JP, Ledinh H, De Roover A et al. Pancreas preservation for pancreas and islet transplantation: A minireview. Transplant Proc 2011;43:3398–3401.

24 Wakayama K, Fukai M, Yamashita K et al. Successful transplantation of rat hearts subjected to extended cold preservation with a novel preservation solution. Transpl Int 2012;25:696–706.

25 Minasian SM, Galagudza MM, Dmitriev YV et al. Preservation of the donor heart: From basic science to clinical studies. Interact Cardiovasc Thorac Surg 2015;20:510–519.

26 Uchida T, Nagayama M, Taira T et al. Optimal temperature range for low-temperature preservation of dissociated neonatal rat cardiomyocytes. Cryobiology 2011;63:279–284.

27 Lu J, Hou R, Booth CJ et al. Defined culture conditions of human embryonic stem cells. Proc Natl Acad Sci USA 2006;103:5688–5693.

28 Orita H, Fukasawa M, Uchino H et al. Long-term hypothermic preservation of cardiac myocytes isolated from the neonatal rat ventricle: A comparison of various crystalloid solutions. Surg Today 1995;25:251–256.

29 Abi-Gerges N, Pointon A, Pullen GF et al. Preservation of cardiomyocytes from the adult heart. J Mol Cell Cardiol 2013;64:108–119.

30 Zhang M, Schulte JS, Heinick A et al. Universal cardiac induction of human pluripotent stem cells in two and three-dimensional formats: Implications for in vitro maturation. Stem Cells 2015;33:1456–1469.

31 Serra M, Correia C, Malpique R et al. Microencapsulation technology: a powerful tool for integrating expansion and cryopreservation of human embryonic stem cells. PLoS One 2011;6:e23212.

32 Wong RCB, Dottori M, Koh KLL et al. Gap junctions modulate apoptosis and colony growth of human embryonic stem cells maintained in a serum-free system. Biochem Biophys Res Commun 2006;344:181–188.

33 Halbach M, Peinkofer G, Baumgartner S et al. Electrophysiological integration and action potential properties of transplanted cardiomyocytes derived from induced pluripotent stem cells. Cardiovasc Res 2013;100:432–440.

34 Elliott DA, Braam SR, Koutsis K et al. NKX2-5(eGFP/w) hESCs for isolation of human cardiac progenitors and cardiomyocytes. Nat Methods 2011;8:1037–1040.

35 Lian X, Zhang J, Azarin SM et al. Directed cardiomyocyte differentiation from human pluripotent stem cells by modulating Wnt/β-catenin signaling under fully defined conditions. Nat Protoc 2013;8:162–175.

36 Skelton RJP, Costa M, Anderson DJ et al. SIRPA, VCAM1 and CD34 identify discrete lineages during early human cardiovascular development. Stem Cell Res (Amst) 2014;13:172–179.

37 Taylor MJ. Biology of cell survival in the cold: The basis for biopreservation of tissues and organs. In: Baust JG, Baust JM, eds. Advances in Biopreservation. Boca Raton, FL: CRC/Taylor & Francis, 2006:15–62.

38 Gherghiceanu M, Barad L, Novak A et al. Cardiomyocytes derived from human embryonic and induced pluripotent stem cells: Comparative ultrastructure. J Cell Mol Med 2011; 15:2539–2551.

39 Grant AO. Cardiac ion channels. Circ Arrhythm Electrophysiol 2009;2:185–194.

40 Lu L, Zhang Q, Timofeyev V et al. Molecular coupling of a Ca2+-activated K+ channel to L-type Ca2+ channels via alpha-actinin2. Circ Res 2007;100:112–120.

41 Ku K, Oku H, Alam MS et al. Prolonged hypothermic cardiac storage with histidine-tryptophan-ketoglutarate solution: comparison with glucose-insulin-potassium and University of Wisconsin solutions. Transplantation 1997; 64:971–975.

42 Wheeler TJ, Chien S. Protection of rat cardiac myocytes by fructose-1,6-bisphosphate and 2,3-butanedione. PLoS One 2012;7:e35023.

43 Orita H, Fukasawa M, Hirooka S et al. Cardiac myocyte functional and biochemical changes after hypothermic preservation in vitro. Protective effects of storage solutions. J Thorac Cardiovasc Surg 1994;107:226–232.

44 See YP, Weisel RD, Mickle DA et al. Prolonged hypothermic cardiac storage for transplantation. The effects on myocardial metabolism and mitochondrial function. J Thorac Cardiovasc Surg 1992;104:817–824.

45 Vettel C, Hottenrott MC, Spindler R et al. Dopamine and lipophilic derivates protect cardiomyocytes against cold preservation injury. J Pharmacol Exp Ther 2014;348:77–85.

46 Schnerch A, Cerdan C, Bhatia M. Distinguishing between mouse and human pluripotent stem cell regulation: The best laid plans of mice and men. Stem Cells 2010;28:419–430.

47 Ernst M, Abu Dawud R, Kurtz A et al. Comparative computational analysis of pluripotency in human and mouse stem cells. Sci Rep 2015;5:7927.

48 Mu J, Li X, Yuan S et al. Comparative study of directional differentiation of human and mouse embryonic stem cells into cardiomyocytes. Cell Biol Int 2014;38:1098–1105.

49 Pontes Soares C, Midlej V, de Oliveira MEW et al. 2D and 3D-organized cardiac cells shows differences in cellular morphology, adhesion junctions, presence of myofibrils and protein expression. PLoS One 2012;7:e38147.

50 Jiang H, Grinnell F. Cell-matrix entanglement and mechanical anchorage of fibroblasts in three-dimensional collagen matrices. Mol Biol Cell 2005;16:5070–5076.

51 Bishopric NH, Andreka P, Slepak T et al. Molecular mechanisms of apoptosis in the cardiac myocyte. Curr Opin Pharmacol 2001;1: 141–150.

52 Rauen U, de Groot H. Cold-induced release of reactive oxygen species as a decisive mediator of hypothermia injury to cultured liver cells. Free Radic Biol Med 1998;24:1316–1323.

53 Stefanovich P, Ezzell RM, Sheehan SJ et al. Effects of hypothermia on the function, membrane integrity, and cytoskeletal structure of hepatocytes. Cryobiology 1995;32:389–403.

54 Boutilier RG. Mechanisms of cell survival in hypoxia and hypothermia. J Exp Biol 2001; 204:3171–3181.

55 Taylor MJ, Rhee P, Chen Z et al. Design of preservation solutions for universal tissue preservation in vivo: Demonstration of efficacy in preclinical models of profound hypothermic cardiac arrest. Transplant Proc 2005;37: 303–307.

56 Bulatovic I, Ibarra C, Österholm C et al. Sublethal caspase activation promotes generation of cardiomyocytes from embryonic stem cells. PLoS One 2015;10:e0120176.

57 Mahler S, Desille M, Frémond B et al. Hypothermic storage and cryopreservation of hepatocytes: The protective effect of alginate gel against cell damages. Cell Transplant 2003;12: 579–592.

58 Ma J, Guo L, Fiene SJ et al. High purity human-induced pluripotent stem cell-derived cardiomyocytes: electrophysiological properties of action potentials and ionic currents. Am J Physiol Heart Circ Physiol 2011;301: H2006–H2017.

59 Dick E, Rajamohan D, Ronksley J et al. Evaluating the utility of cardiomyocytes from human pluripotent stem cells for drug screening. Biochem Soc Trans 2010;38:1037–1045.

60 Wheeler TJ, Wiegand CB, Chien S. Fructose-1,6-bisphosphate enhances hypothermic preservation of cardiac myocytes. J Heart Lung Transplant 2005;24:1378–1384.

61 Fagbemi OS, Northover BJ. Effect of protein kinase C inhibitors and 2,3-butanedione monoxime on the long-term hypothermic preservation of isolated rat hearts. Clin Sci (Lond) 1996;91:745–754.

62 Jabbour A, Gao L, Kwan J et al. A recombinant human neuregulin-1 peptide improves preservation of the rodent heart after prolonged hypothermic storage. Transplantation 2011;91:961–967.

63 Dai J, Meng Q. Differential function of protective agents at each stage of the hypothermic preservation of hepatocytes. J Biochem 2011;149:739–745.

64 Bauer M, Kang L, Qiu Y et al. Adult cardiac progenitor cell aggregates exhibit survival benefit both in vitro and in vivo. PLoS One 2012;7: e50491.

See www.StemCellsTM.com for supporting information available online.